JJEE
Volume 11 | Number 3 | September 2025 | Pages 529-545

Jordan Journal of Electrical Engineering

ISSN (print): 2409-9600, ISSN (online): 2409-9619

Homepage: jjee.ttu.edu.jo

Enhancing Performance of Distance Relay by Reducing Oscillations in Impedance Calculation Utilizing Modified Least-Squares Algorithm

Amir Ghorbani[1*]

[1] Department of Electrical Engineering, Ab. C., Islamic Azad University, Abhar, Iran
E-mail: amirghorbani.elec@gmail.com

Received: Apr 23, 2025 *Revised: Jun 15, 2025* *Accepted: Sep 02, 2025* *Available online: Nov 27, 2025*

***Abstract*—** Distance relays serve as critical protection devices for transmission lines in power systems by calculating line impedance up to fault locations. Accurate impedance measurement is essential, as relay malfunction can lead to partial or complete grid blackouts. These relays utilize voltage and current phasors from Phasor Measurement Units (PMUs) for impedance computation. Conventional methods employing Discrete Fourier Transform (DFT) techniques - including Full-Cycle DFT (FCDFT) and Half-Cycle DFT (HCDFT), often combined with mimic filters - exhibit two significant limitations: sensitivity to source impedance and substantial impedance oscillations that frequently cause relay malfunction. This paper presents a modified Least-Squares (LES) algorithm and compares its performance against FCDFT and HCDFT-based phasor estimation with mimic filters. Simulation results demonstrate that the proposed method significantly reduces impedance oscillations in relay measurements, eliminating malfunction during fault diagnosis. Furthermore, the algorithm maintains consistent accuracy regardless of source impedance variations, performing reliably both with and without source impedance present. All simulations were implemented in MATLAB/Simulink to validate these findings.

***Keywords*—** Distance relay; Phasor measurement units (PMUs); Least-squares (LES) algorithm; Mimic filter; Full-cycle discrete Fourier transform (FCDFT); Half-cycle discrete Fourier transform (HCDFT).

1. INTRODUCTION

Transmission lines constitute the primary power delivery infrastructure, responsible for the efficient transmission of electrical energy [1, 2]. Their protection is critical, as they experience higher fault susceptibility compared to other power system components [3–8]. A widely adopted protection solution employs distance relays, which operate by measuring the impedance between the relay location and the fault point. For accurate impedance calculation, these relays require precise voltage and current measurements at their installation point. The protection process begins with signal conditioning: The raw signals from current and voltage transformers are first scaled to levels compatible with relay input requirements (Fig. 1). Subsequently, these analog signals undergo anti-aliasing filtering to remove harmonic components before analog-to-digital conversion.

Following signal conditioning, the phasors of the voltage and current signals are extracted using established techniques, with Discrete Fourier Transform (DFT) analysis representing the method illustrated in Fig. 1 [9–13]. This phasor estimation process is critical, as its accuracy directly governs the operational reliability of distance relays. Finally, the calculated phasors are applied to the relay's impedance computation algorithm, allowing the relay to detect and locate faults along the transmission line via the measured impedance [14-17].

* Corresponding author
DOI: https://doi.org/10.5455/jjee.204-1745413560

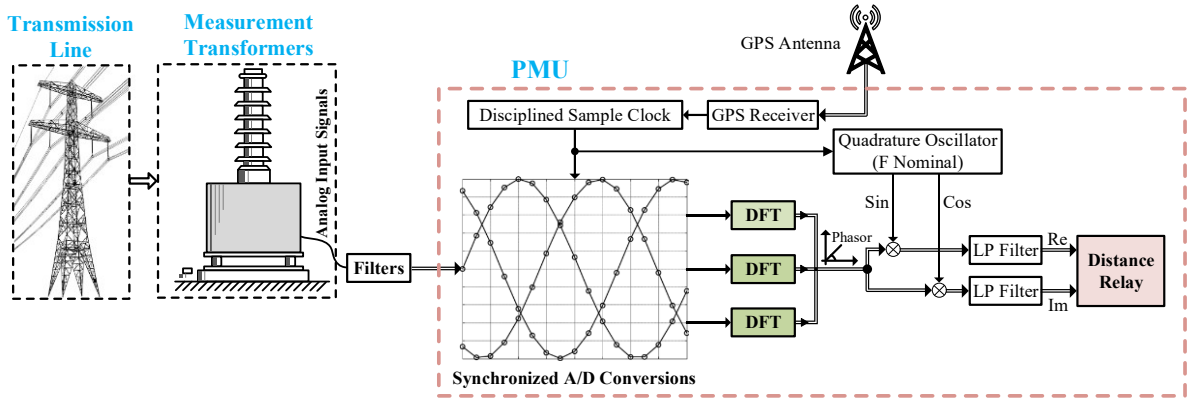

Fig. 1. Essential elements of the distance relay.

During power system faults, transient phenomena distort measurements, leading to erroneous impedance calculations by distance relays. These distorting factors include:

1. The decaying DC offset (caused by the system's resistive-inductive nature)
2. Harmonic components
3. Off-nominal frequency elements

Notably, while these transients severely corrupt current waveforms, their impact on voltage signals is comparatively negligible. During transmission line faults, the DC offset in fault current introduces significant errors in phasor estimation. Failure to eliminate this component results in calculated phasors deviating substantially from actual values, compromising relay accuracy [18-20].

In modern power systems, numerous digital algorithms have been proposed for phasor estimation [15-23], with DFT-based methods emerging as the predominant choice in practical applications [24]. Their widespread adoption stems from straightforward implementation and low computational overhead. Nevertheless, a critical limitation arises during faults: the exponentially decaying DC component in current signals introduces errors in DFT calculations, causing distance relays to either overreach or underreach [25]. This inherent drawback represents a major obstacle for accurate fundamental-frequency phasor estimation and remains an active research challenge.

Multiple techniques have been developed to mitigate the phasor estimation errors caused by exponentially decaying DC components. These methods focus on improving phasor accuracy by minimizing the influence of DC offsets, employing either post-processing techniques or extended analysis windows. However, their performance depends not just on precise fundamental-frequency estimation but also on effective suppression of interfering frequency components. Moreover, the speed of response is directly affected by the length of the analysis window.

Conventional solutions have proposed modified Fourier-based approaches, such as full-cycle and half-cycle DFT variants, to compensate for phasor errors induced by decaying DC components in DFT outputs [26–29]. The fundamental difference between these methods lies in their harmonic rejection capability. Furthermore, an improved Fourier-based approach, the Inverse DFT (IDFT), has demonstrated effectiveness in mitigating decaying DC component effects [30]. Beyond conventional approaches, researchers have developed multiple advanced solutions, including least-squares (LES) algorithms, Fourier-wavelet hybrid methods, empirical mode decomposition (EMD), and cosine filtering architectures [21, 27, 30–34]. State-of-the-art

implementations now integrate artificial neural networks (ANNs) into distance relay systems [35–39]. Advances in data science have renewed interest in these techniques, yielding innovative phasor estimation and impedance measurement algorithms for modern protection schemes [15, 40-43]. While these methods show promising results, they require both initial training and continuous adaptation, potentially introducing errors during initialization or ongoing operation.

Consequently, their reliability is highly dependent on the quality of training data and procedures. Traditional approaches, such as mimic circuits, have been widely used to mitigate DC component effects [28, 44]. However, mimic filters only achieve optimal performance when their time constant matches the system's actual DC offset time constant [44]. This alignment depends on the X/R ratio of the burden circuit being equal to the system's X/R ratio. Since the X/R ratio varies with network switching conditions and fault arc resistance, the filter's effectiveness becomes scenario dependent.

Optimal performance occurs when the mimic filter's time constant equals the current waveform's time constant. As demonstrated in [4], this can be achieved by dynamically adjusting the filter's time constant to match the sampled waveform. The research shows that FCDFT-based mimic filters outperform HCDFT variants using identical filter parameters. Nevertheless, as reported in [23], even with improved phasor estimation, the resulting impedance measurements exhibit oscillations near steady-state values.

These fluctuations degrade distance relay accuracy, particularly for zone-1 protection. In conventional implementations, zone-1 relays typically issue trip commands instantaneously upon detecting impedance within their operating characteristic. This immediate response makes them vulnerable to impedance oscillations, potentially causing malfunction during transient conditions.

This study presents a novel first-order adaptive least squares (ALS) algorithm integrated with a dynamically tuned mimic filter, wherein the time constant is continuously updated in real-time. The performance of the proposed method is systematically evaluated against the technique described in [13], with comparative results detailed in subsequent sections. Our findings demonstrate that the ALS-based approach achieves superior performance, substantially minimizing oscillations in both impedance calculations and phasor estimates relative to the reference method [13].

Beyond distance protection, this method exhibits potential for broader application in other impedance-based relays, including loss-of-excitation (LOE) protection systems for synchronous generators [45–47].

2. FIRST-ORDER LES ALGORITHM

The measured current signal is assumed to include a damped DC component, the fundamental component, and harmonic components (up to the nth order). Thus, it can be expressed as follows [48]:

$$i(t) = k_0 e^{\frac{-t}{\tau}} + k_1 \sin(\omega_0 t + \theta_1) + \ldots + k_n \sin(n\omega_0 t + \theta_n) \quad (1)$$

In Eq. (1), τ, ω, and k_n are the time constant of the DC component, angular frequency, and constant coefficients, respectively. Eq. (2) is obtained by expanding Eq. (1) as follows:

$$i(t) = k_0 e^{\frac{-t}{\tau}} + (k_1 \cos\theta_1) \sin\omega_0 t + (k_1 \sin\theta_1) \cos\omega_0 t + \cdots + (k_n \cos\theta_n) \sin n\omega_0 t + (k_n \sin\theta_n) \cos n\omega_0 t \quad (2)$$

Based on Eq. (2), the instantaneous value of the current signal at moment $t=t_1$ is expressed as follows:

$$i(t_1) = a_{11}x_1 + a_{12}x_2 + \ldots a_{1(2n)}x_{2n} + a_{1(2n+1)}x_{2n+1} \quad (3)$$

The coefficients a_{11} to $a_{1(2n+1)}$ in Eq. (3) pertain to the sampling time:

$$a_{11} = e^{\frac{-t_1}{\tau}}, a_{12} = \sin \omega_0 t_1$$
$$a_{1(2n)} = \sin n\omega_o t_1, a_{1(2n+1)} = \cos n\omega_0 t_1 \quad (4)$$

And the coefficients from x_1 to $x_{(2n+1)}$ are expressed as follows:

$$x_1 = k_0, x_2 = k_1 \cos\theta_1, \ldots, x_{2n+1} = k_n \sin\theta_n \quad (5)$$

Using m samples of the input signal that have been measured at predetermined and known times, Eq. (5) can be expressed in the following matrix form:

$$[A]_{m\times(2n+1)} \times [X]_{2n+1} = [S]_{m\times 1} \quad (6)$$

In Eq. (6), the vector of unknowns X is:

$$[A]' = \left[[A]^T[A]\right]^{-1}[A]^T$$
$$[X] = \left[A'\right][S] \quad (7)$$

The matrix [A]' is the pseudo-inverse of matrix A. The amplitude and phase of the signal's fundamental component are derived from vector X, specifically using elements x_2 and x_3. Fig. 2 illustrates the block diagram for computing the amplitude and phase of the sampled signal. In this diagram, the transfer functions G1(z) and G2(z), corresponding to the first order least squares error algorithm, are defined as follows.

$$G1(z) = \sum_{i=0}^{i=m-1} A'(2, m-i)z^{-i}$$
$$G2(z) = \sum_{i=0}^{i=m-1} A'(3, m-i)z^{-i} \quad (8)$$

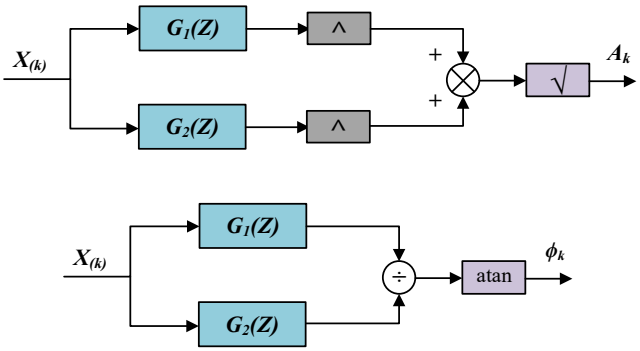

Fig. 2. Block diagram of estimating the amplitude and phase of a sampled signal $X_{(k)}$.

Regarding Eq. (8), the parameter m represents the number of samples per cycle. For this study, a value of m = 32 samples per cycle was chosen. The frequency response of the functions G1(z) and G2(z) corresponding to the modified and conventional first-order LES algorithm combined with an adapted mimic filter is shown in Fig. 3. The integration of the proposed phasor estimation method with the adaptive mimic filter follows an approach similar to that described in [13], where two methods—FCDFT and HCDFT—were combined with the mimic filter. To avoid redundancy, the implementation details of this integration are not repeated here, as they are thoroughly presented in [13]. In Fig. 3, the x-axis is normalized around the main frequency. The results show that proposed method removes the DC component more effectively than the conventional first order least squares method. Three types of systems were examined: First, a system where the source impedance was set to zero (with the source

impedance considered negligible). Second, a system where the voltage was measured after the source impedance (with the source impedance accounted for). Third, a system identical to the second type, but with current and voltage signals modeled with high THD.

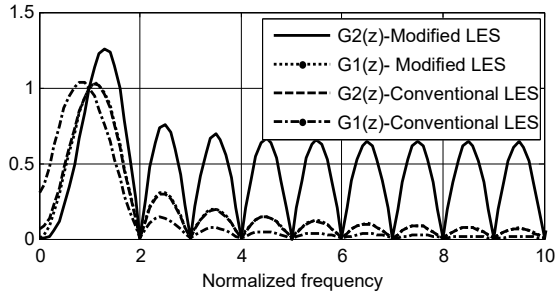

Fig. 3. Frequency response of functions G1(z), G2(z) related to modified and conventional first-order LES methods combined with an adapted mimic filter.

2.1. Without Source Impedance

The system considered in this section, modeled in MATLAB/Simulink, is shown in Fig. 4. The power switch closes after 4 cycles, and the total simulation time equals 12 cycles, with m=32 samples per cycle. The time constant of the sampled signal is obtained using the method described in reference [13] for both the mimic filter and the first order least squares method. The voltage and current waveforms are shown in Figs. 5 and 6, respectively, while Fig. 7 presents the Fourier analysis of the current waveform. The decaying DC component is clearly visible in the current waveform and persists for nearly four cycles.

To evaluate the mimic filter's influence, this section presents results omitting the adapted mimic filter. Fig. 8 compares current phasor magnitudes calculated using four methods: FCDFT, HCDFT, conventional LES, and modified LES (all without the mimic filter). The results demonstrate that FCDFT, HCDFT, and conventional LES exhibit oscillations around the current phasor's final value when the mimic filter is not used. The HCDFT method shows significantly greater oscillations than the other methods. The results demonstrate that the modified LES method achieves the lowest oscillation amplitude compared to the other methods. Even without the adapted mimic filter, this method maintains an acceptable accuracy level.

Fig. 9 shows the apparent impedance magnitude calculated by the relay. The results confirm that the modified LES method exhibits significantly smaller oscillations around its final value compared to the other three methods. Distance relays operate based on a two-dimensional impedance zone (such as MHO relay): when the calculated apparent impedance enters this zone, the relay initiates a trip response. Consequently, reduced oscillations in impedance calculations directly improve operational accuracy. To further demonstrate this effect, Fig. 10 compares the apparent impedance computed using all four methods. The modified LES method yields the lowest oscillations, while the HCDFT method produces the most severe oscillations. Critically, Fig. 10 reveals that excessive oscillations may cause intermediate impedance values to falsely enter the operating zone, while the actual steady-state impedance remains outside it. Such scenarios risk relay malfunction, which the modified LES method effectively mitigates through its oscillation suppression.

The following analysis presents results obtained by combining the four methods (FCDFT, HCDFT, conventional LES, and modified LES with the adaptive mimic filter). Fig. 11 displays the current phasor magnitudes calculated using these methods when employing the

adaptive mimic filter. Two key observations emerge from these results: first, the adaptive mimic filter significantly reduces oscillations across all methods; second, the modified LES method consistently outperforms the other approaches.

Figs. 12 and 13 present the apparent impedance magnitude and relay output impedance, respectively. The modified LES method demonstrates notably smaller oscillations around the final impedance value in Fig. 13, leading to substantially improved relay accuracy. Comparative analysis of Figs. 10 and 13 reveals that the modified LES method maintains superior performance regardless of whether the adaptive mimic filter is implemented.

To specifically evaluate the filter's impact on the modified LES method, Fig. 14 compares results with and without the adaptive mimic filter. This comparison confirms that the filter reduces impedance oscillations to negligible levels in the modified LES method. Furthermore, for the fault scenario depicted in Fig. 4, the distance relay accurately calculates the final apparent impedance value, validating the method's precision.

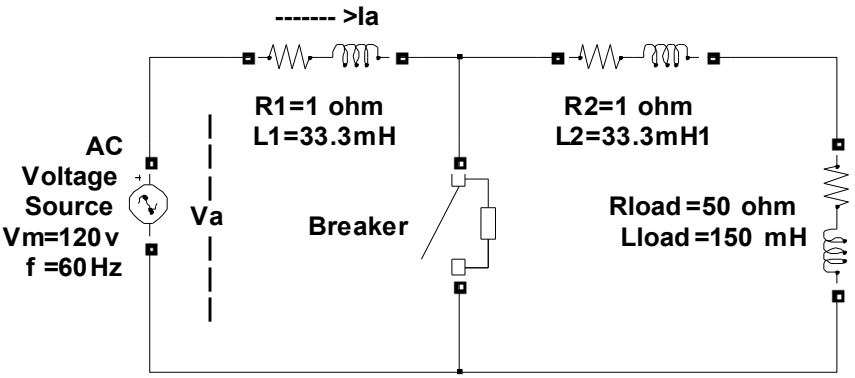

Fig. 4. Modeled power system without considering source impedance.

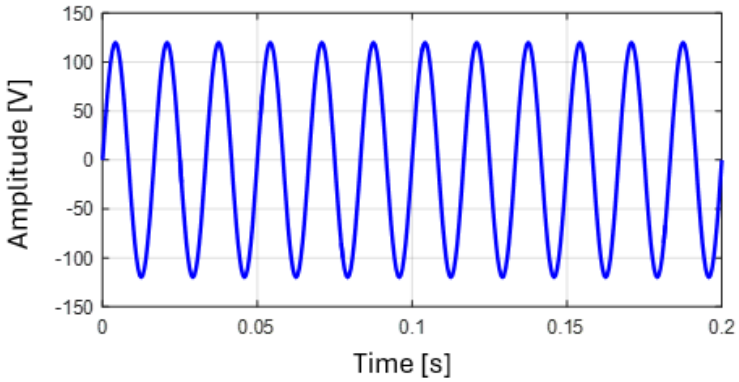

Fig. 5. Sampled voltage waveform.

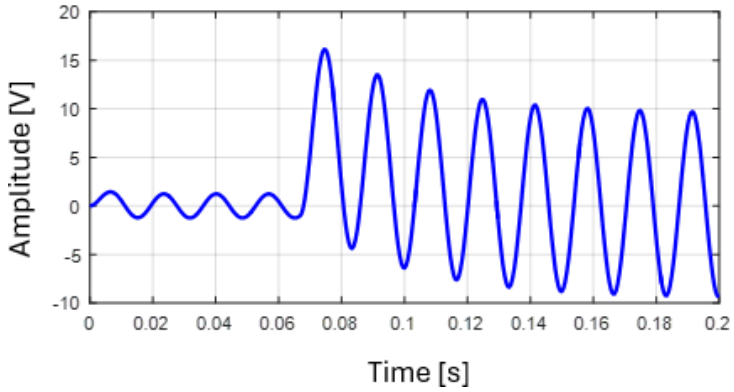

Fig. 6. Sampled current waveform.

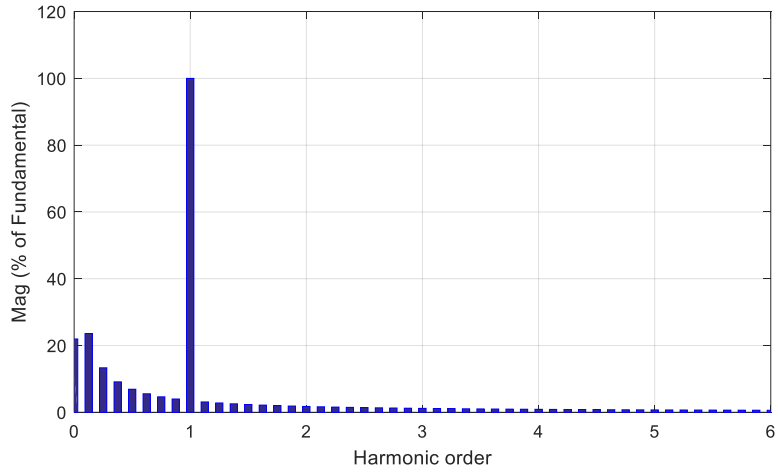

Fig. 7. Fourier analysis of current waveform.

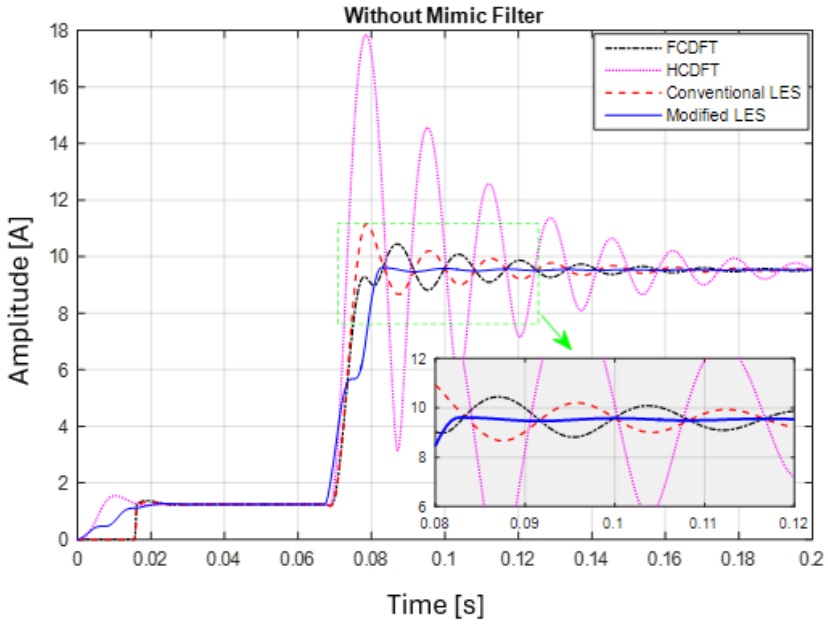

Fig. 8. The magnitude of the fundamental component of the calculated current phasor.

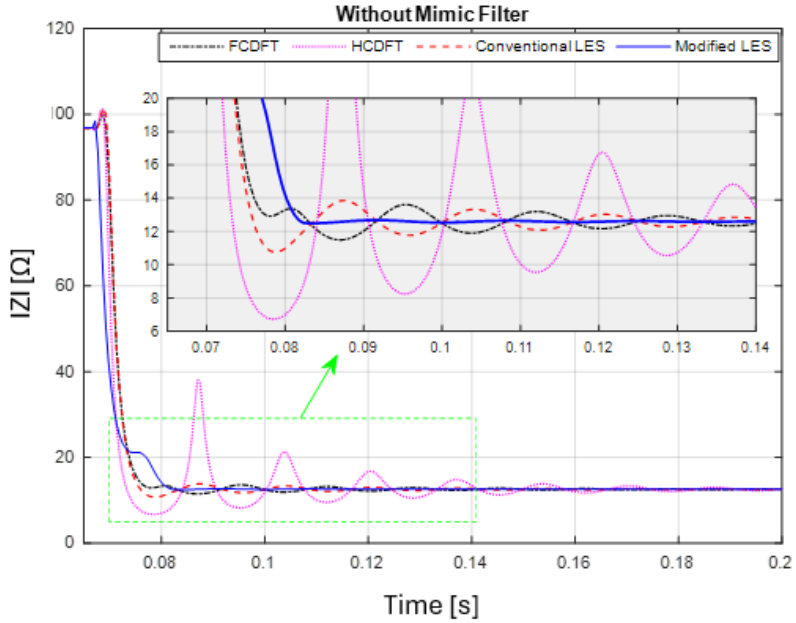

Fig. 9. The magnitude of the calculated apparent impedance by relay.

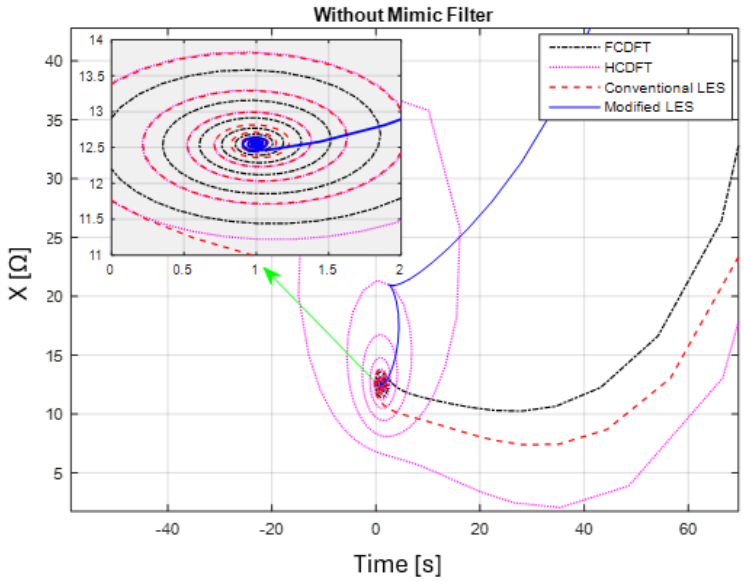

Fig. 10. The calculated apparent impedance by distance relay.

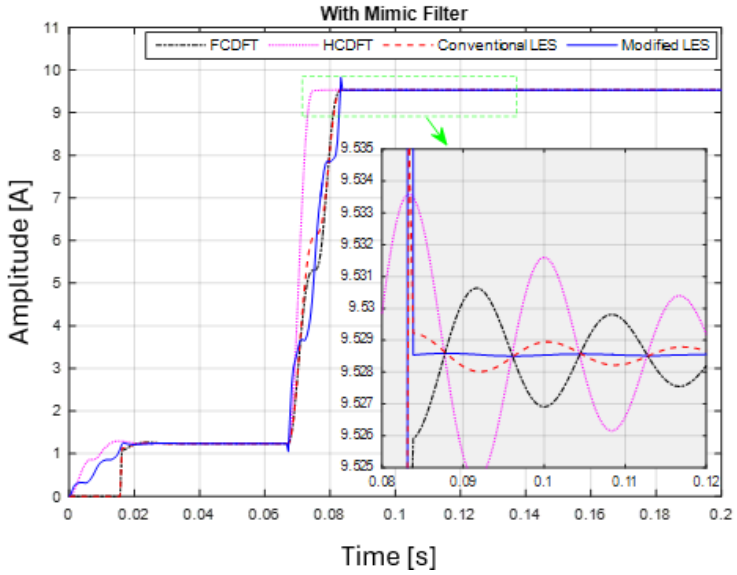

Fig. 11. The magnitude of the fundamental component of the calculated current phasor.

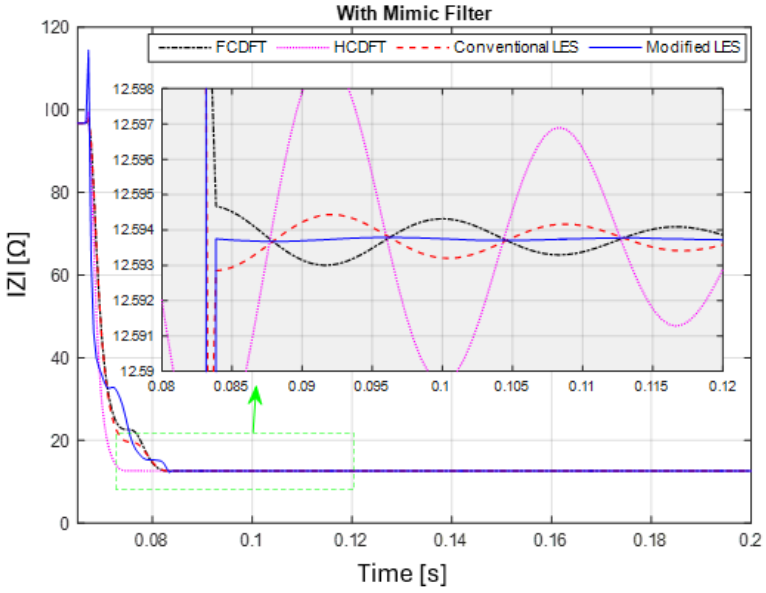

Fig. 12. The magnitude of the calculated apparent impedance by relay.

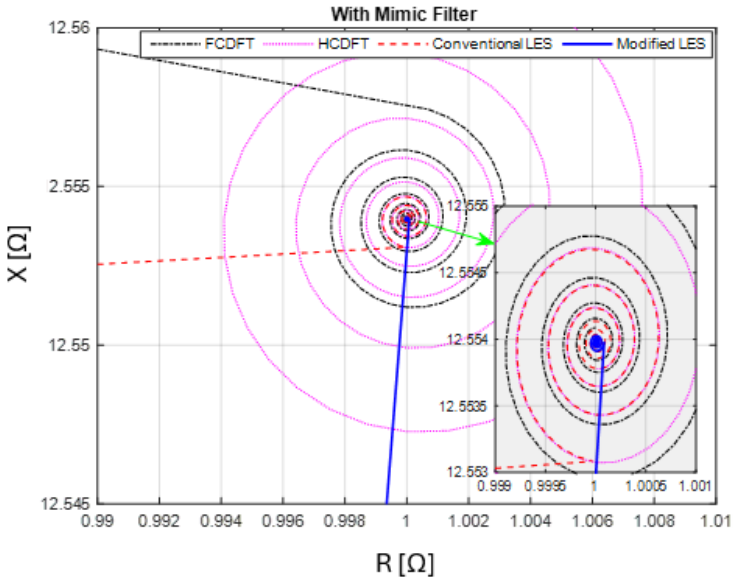

Fig. 13. The calculated apparent impedance by distance relay.

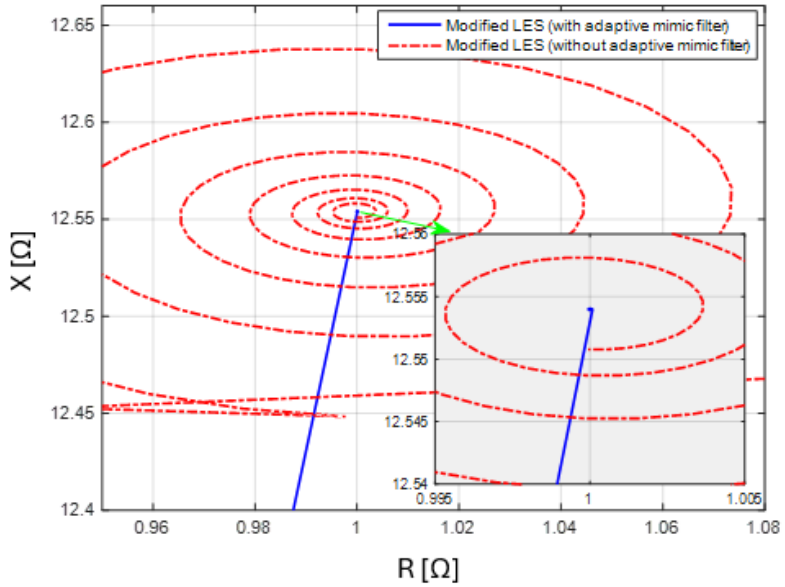

Fig. 14. The calculated apparent impedance by distance relay.

2.2. With Source Impedance

In this section, it is assumed that the source impedance is behind the measured voltage. The system was implemented in the MATLAB/Simulink environment, as shown in Fig. 15. The source impedance values are R = 1.5 Ω and L = 30 mH, with the fault occurring after four cycles. The time constant was obtained using the method described in reference [13]. This same value was then applied to both the mimic filter and the first-order least squares method after fault inception. The magnitude of the measured apparent impedance is calculated as follows:

$$\sqrt{((.0333 \times 120 \times \pi)^2 + 1)} = 12.5935\ \Omega \quad (9)$$

The sampled voltage and current waveforms are shown in Fig. 16. These results clearly indicate that the DC component cannot be neglected. When the voltage phasor is calculated using conventional FCDFT or HCDFT methods without mimic filtering, this approach increases oscillations in the apparent impedance around its final value. As demonstrated in earlier sections, the absence of the mimic filter causes greater oscillations in the FCDFT, HCDFT,

and conventional LES methods. For subsequent analyses, all presented results incorporate the mimic filter, while results without the filter have been omitted for conciseness. The results presented combine the four methods (FCDFT, HCDFT, conventional LES, and modified LES) with the adaptive mimic filter. Fig. 17 shows the current phasor magnitude calculated by these methods. The results demonstrate that the adaptive mimic filter reduces oscillations in all four methods, with the modified LES method maintaining superior performance. Figs. 18 and 19 present the apparent impedance magnitude and relay output impedance, respectively. Fig. 18 confirms that the modified LES method yields significantly smaller oscillations around the final impedance value compared to the other methods, leading to improved relay accuracy. Comparative analysis of Figs. 10 and 19 shows that the modified LES method produces the least impedance oscillations regardless of source impedance presence. For the fault scenario in Fig. 15, the distance relay correctly calculates the final apparent impedance value, validating the method's precision.

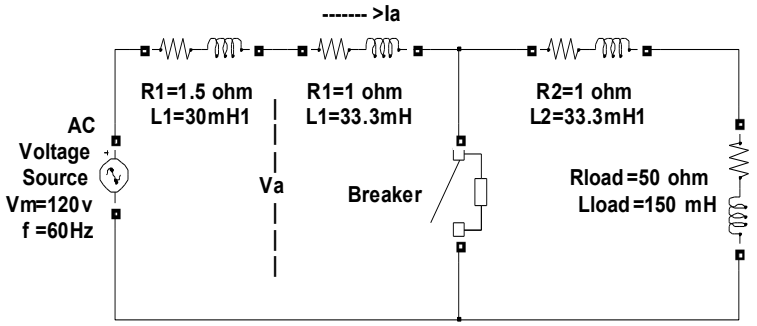

Fig. 15. Modeled power systems with considering source impedance.

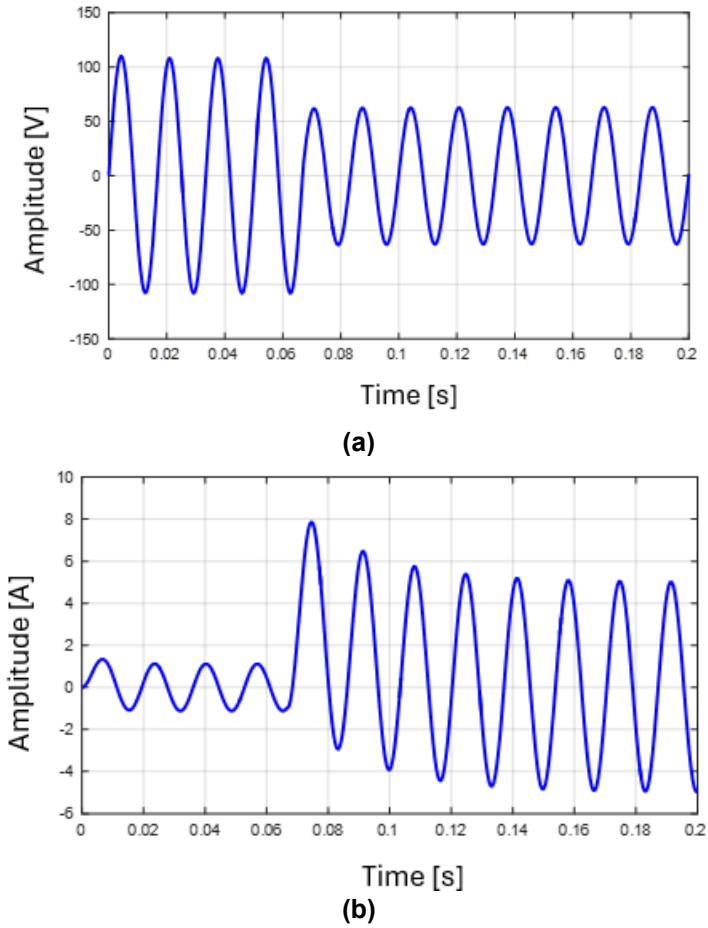

Fig. 16. Sampled measured signals: a) voltage; and b) current waveform.

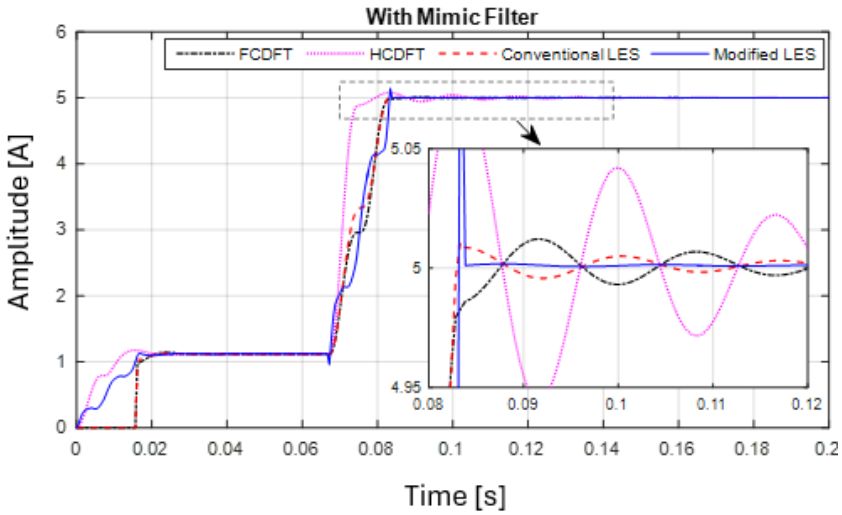

Fig. 17. The magnitude of the fundamental component of the calculated current phasor.

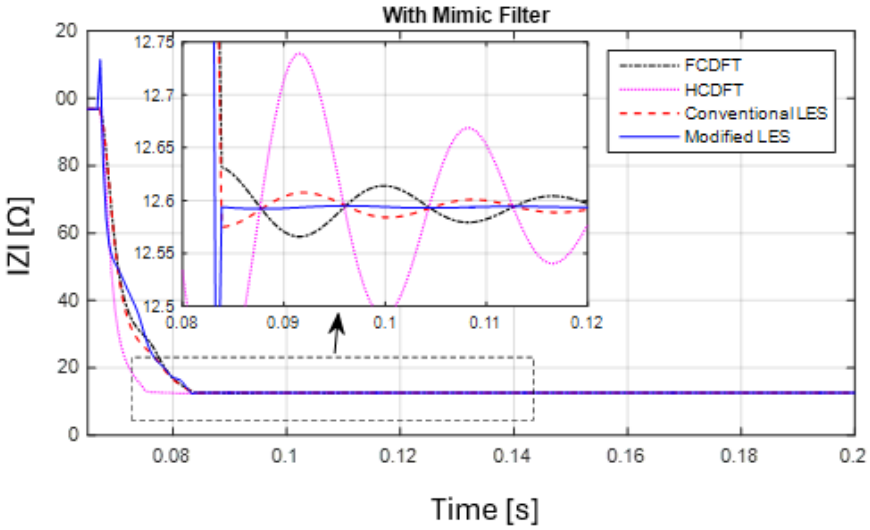

Fig. 18. The magnitude of the calculated apparent impedance by relay.

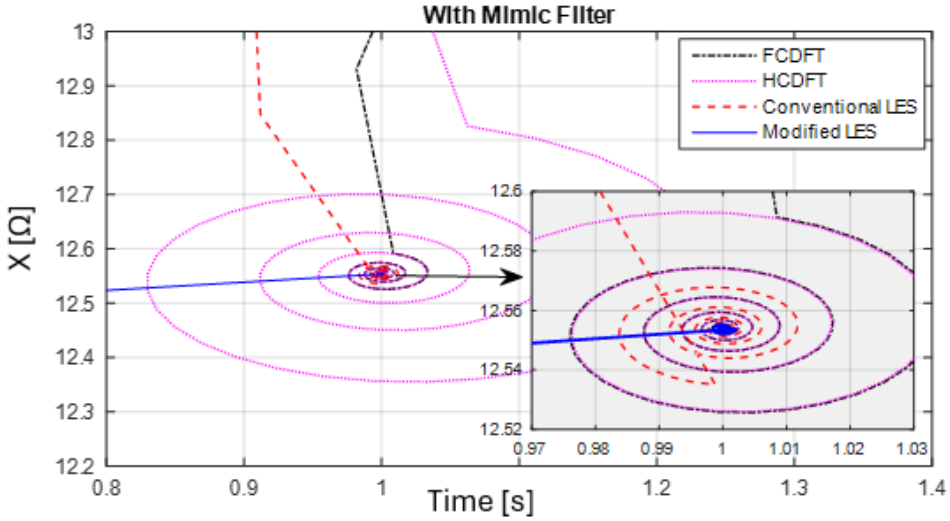

Fig. 19. The calculated apparent impedance by distance relay.

2.3. With Source Impedance and High THD Signals

In this phase of the study, the input voltage was configured to induce high total harmonic distortion in both voltage and current waveforms. This approach enables direct comparison of

harmonic mitigation performance across the analyzed methods. The test system is shown in Fig. 20, with the input voltage defined as (fundamental frequency = 60 Hz):

$$V(t) = 120\sin(\omega t) + 25\sin(2\omega t + pi/3) + 20\sin(3\omega t) + 15\sin(4\omega t) + 10\sin(5\omega t) \quad (10)$$

The voltage and current waveforms, along with their Fourier analysis results, are presented in Figs. 21 through 24. The Fourier analysis of the current waveform reveals a total harmonic distortion (THD) of 14.04%. To objectively compare the harmonic elimination capabilities of the investigated methods, a representative signal segment was selected for analysis.

The following results were obtained by applying the four methods (FCDFT, HCDFT, conventional LES, and modified LES) in combination with the adaptive mimic filter. Fig. 25 presents the current phasor magnitudes calculated using these methods. Detailed examination of the current phasors in Fig. 25 reveals that the HCDFT method, when combined with the adaptive mimic filter, exhibits significant oscillations because of its inability to eliminate even-order harmonics.

Figs. 26 and 27 show the apparent impedance magnitude and relay output impedance, respectively. Fig. 26 demonstrates that the modified LES method produces substantially smaller oscillations around the final impedance value compared to the other methods, leading to enhanced relay accuracy. Consistent with previous results in Figs. 10 and 19, the modified LES method maintains superior performance in both cases (with and without source impedance), as evidenced in Fig. 27. For the fault location presented in Fig. 27, the distance relay accurately calculates the final apparent impedance value, confirming the method's reliability.

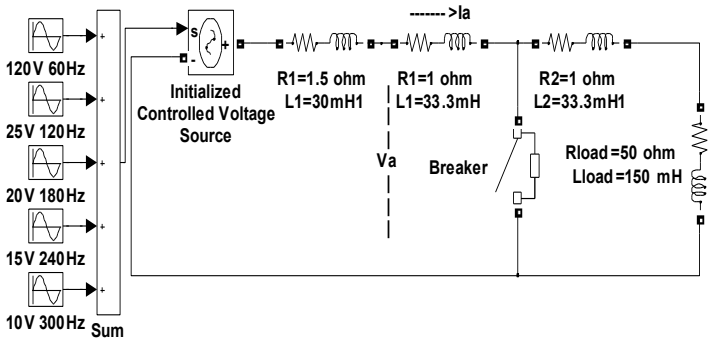

Fig. 20. Modeled power system with considering source impedance and high THD signals.

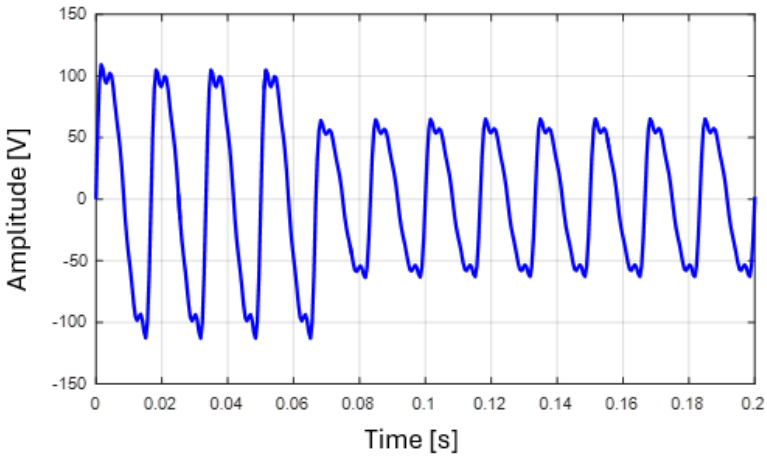

Fig. 21. Sampled voltage waveform.

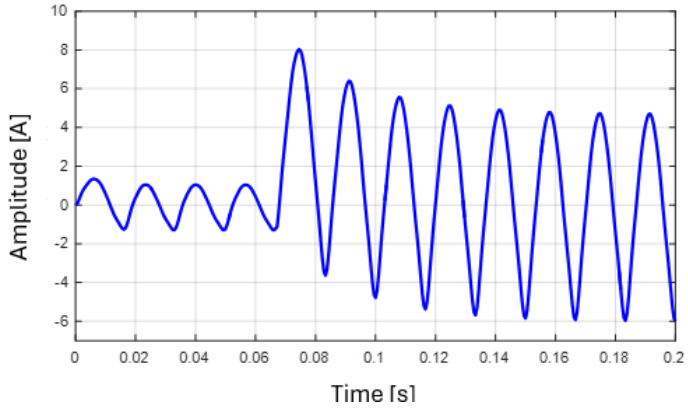

Fig. 22. Sampled current waveform.

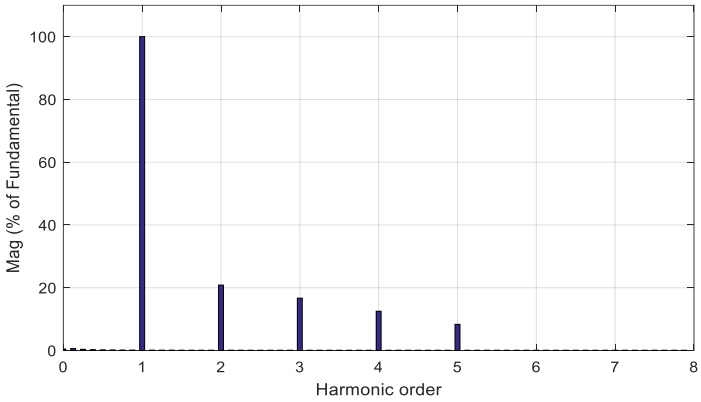

Fig. 23. Fourier analysis of voltage waveform.

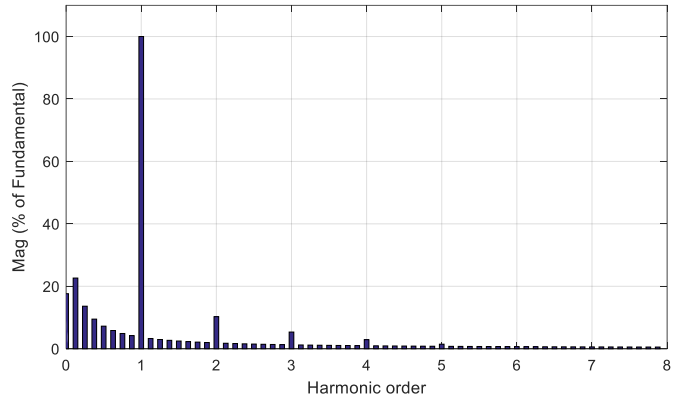

Fig. 24. Fourier analysis of current waveform.

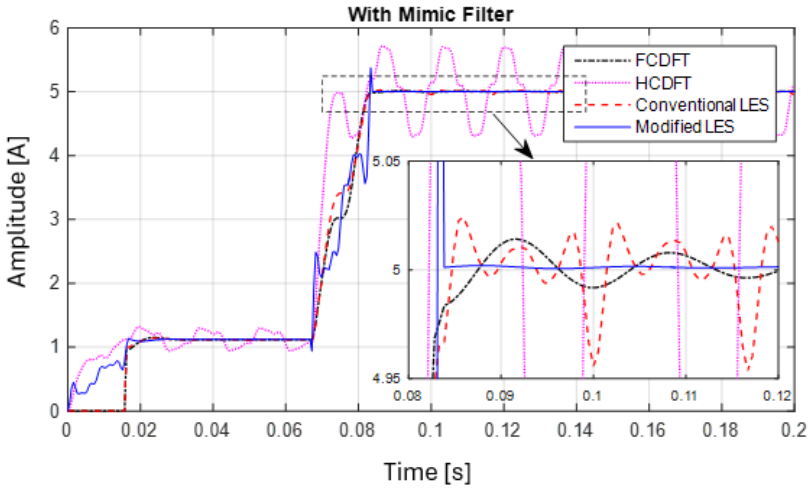

Fig. 25. The magnitude of the fundamental component of the calculated current phasor.

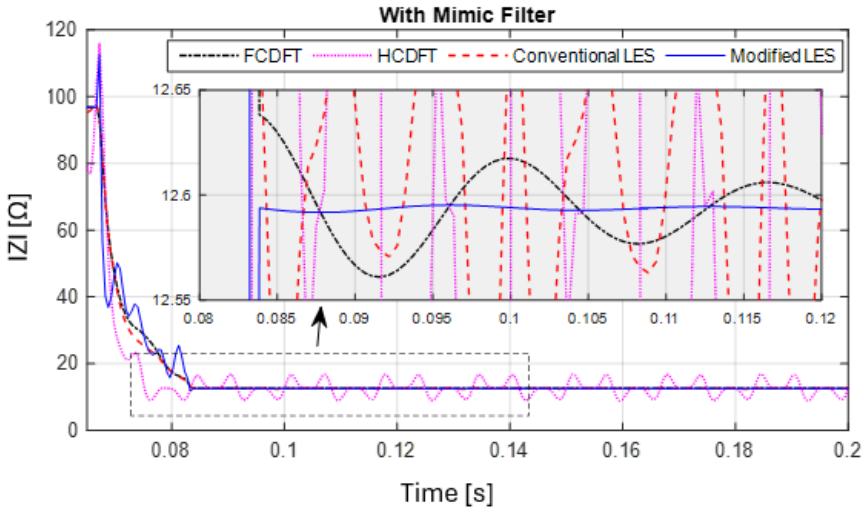

Fig. 26. The magnitude of the calculated apparent impedance by relay.

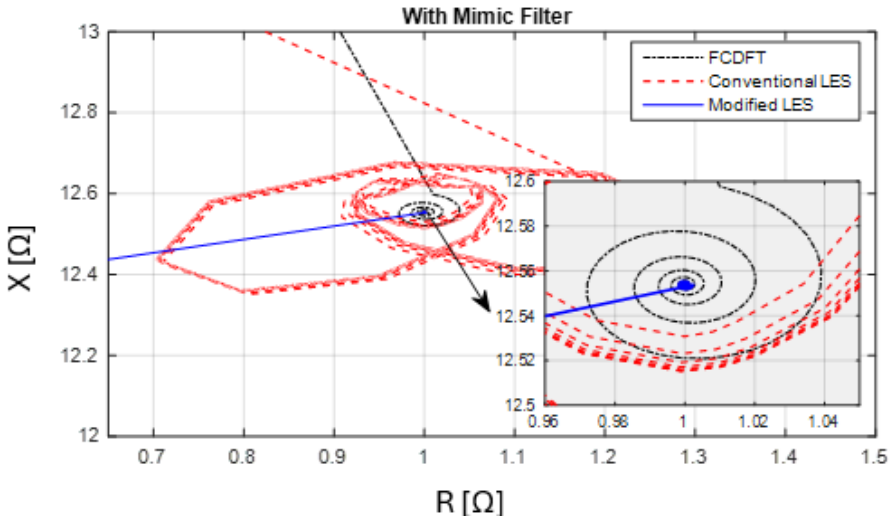

Fig. 27. The calculated apparent impedance by distance relay.

3. CONCLUSIONS

This study demonstrates that the first order least squares method integrated with the adaptive mimic filter achieves superior measurement accuracy relative to conventional half-cycle and full-cycle Fourier methods employed in typical PMUs. The findings reveal that the proposed method:

- Provides highly accurate apparent impedance detection in MHO relays, effectively eliminating erroneous samples from relay operating zones
- Prevents distance relay malfunction and subsequent unnecessary tripping of transmission line loads
- Is readily applicable to other impedance-based protection schemes, including loss-of-excitation (LOE) relays for synchronous generators

The combined approach of adaptive filtering and least squares estimation addresses critical limitations of Fourier-based methods, particularly in handling DC offsets and harmonic distortion.

REFERENCES

[1] W. Malska, "Analysis of current ampacity of the 110 kV overhead transmission line using a multiple regression model," *Electric Power Systems Research*, vol. 236, 2024, doi: 10.1016/j.epsr.2024.110939.

[2] H. Chen, Z. Hu, Z. Wang, J. Tan, X. Xu, Z. Sun, "New method for live line measuring the zero-sequence distribution parameters for partial parallel double-circuit transmission lines," *International Journal of Electrical Power & Energy Systems,* vol. 169, 2025, doi: 10.1016/j.ijepes.2025.110763.

[3] A. Ghorbani, M. Sanaye-Pasand, H. Mehrjerdi "Accelerated distance protection for transmission lines based on accurate fault location," *Electric Power Systems Research*, vol. 193, 2021, doi: 10.1016/j.epsr.2021.107021.

[4] S. Azizi, M. Sun, G. Liu, M. Popov, V. Terzija, "High-speed distance relaying of the entire length of transmission lines without signaling," *IEEE Transactions on Power Delivery*, vol. 35, no. 4, pp. 1949–1959. 2020, doi: 10.1109/TPWRD.2019.2957302.

[5] G. Kapoor, "A mathematical morphology-based fault detection and faulty phase categorization scheme for the protection of six-phase transmission line," *Jordan Journal of Electrical Engineering*, vol. 6, n. 1, 2020, doi: 10.5455/jjee.204-1581015401.

[6] A. Ghorbani, H. Mehrjerdi, "Distance protection with fault resistance compensation for lines connected to PV plant", *International Journal of Electrical Power & Energy Systems*, vol. 148, 2023, doi: 10.1016/j.ijepes.2023.108976.

[7] M. Araújo, E. Batista, "A practical first-zone distance protection formulation based on the nominal л transmission line model", *Electric Power Systems Research*, vol. 246, 2025, doi: 10.1016/j.epsr.2025.111665.

[8] A. Kumar, M. Ramesha, E. Kiran, M. Kumar, M. Nagaraju, M. Chakravarthy, B. Gururaj, "Location of faults in six phase transmission line using a neuro fuzzy system," *Jordan Journal of Electrical Engineering*, vol. 10, n. 3, 2024, doi: 10.5455/jjee.204-1694875095.

[9] M. Arpanahi, M. Fini, M. Khoshnama, A. Ghorbani, "A fast and accurate bi-level fault location method for transmission system using single ended phasor measurements," *Electric Power Systems Research*, vol. 210, 2022, doi: 10.1016/j.epsr.2022.108110.

[10] *C37.118-IEEE standard for synchro phasor measurements for power systems*, 2005, https://ieeexplore.ieee.org/document/6111219.

[11] A. Ghorbani, H. Mehrjerdi, A. Iqbal "Modeling of digital distance relay in emtpworks considering protective zones and trip characteristics," International Conference on Smart Grid and Renewable Energy, 2019, doi: 10.1109/SGRE46976.2019.9021049.

[12] M. Nemati, M. Bigdeli, A. Ghorbani, H. Mehrjerdi, "Accurate fault location element for series compensated double-circuit transmission lines utilizing negative-sequence phasors," *Electric Power Systems Research*, vol. 194, 2021, doi: 10.1016/j.epsr.2021.107064.

[13] Chi-Shan Yu, "A discrete fourier transform-based adaptive mimic phasor estimator for distance relaying applications," *IEEE Transactions on Power Delivery*, vol. 21, pp. 1836–1846, 2006, doi: 10.1109/TPWRD.2006.874609.

[14] M. Nemati, M. Bigdeli, A. Ghorbani, "Impedance-based fault location algorithm for double-circuit transmission lines using single-end data," *Journal of Control, Automation and Electrical Systems*, vol. 31, n. 5, 2020, doi: 10.1007/s40313-020-00620-w.

[15] R. Pujari, M. Alam, "Distance relaying for the protection of modern power system networks," *IEEE Access*, vol. 13, 2025, doi: 10.1109/ACCESS.2025.3539919.

[16] A. Garzón, D. Celeita, G. Ramos, M. Petit, T. Le, J. Hoyos, Al. Bach, "Comparative analysis of impedance and time-domain protection in HVAC and HVDC interconnected systems: A case study in Colombia," *e-Prime-Advances in Electrical Engineering, Electronics and Energy*, vol. 11, 2025, doi: 10.1016/j.prime.2024.100880.

[17] M. Alsharari, M. Ahmed, W. Abu Shehab, S. Ali, "Evaluation of harmonic currents and network impedance using norton model in an unidentified network configuration," *Jordan Journal of Electrical Engineering*, vol. 10, n. 1, 2024, doi: 10.5455/jjee.204-1686253514.

[18] A. Mendez, J. Castañón, M. Arrieta, P Buendia, C Torres, CToledo-Santos, VVelasco, F. Zelaya-A, G. Mejia-Ruiz, "Two effective methods for impedance estimation in distance relays based on the DC offset removal," *Electric Power Systems Research*, vol. 194, 2021, doi: 10.1016/j.epsr.2021.107102.

[19] A. Srivastava, L. Tuan, D. Steen, O. Carlson, O. Mansour, D. Bijwaard, "Dynamic state estimation based transmission line protection scheme: Performance evaluation with different fault types and conditions," *International Journal of Electrical Power & Energy Systems*, vol. 148, 2023, doi: 10.1016/j.ijepes.2023.108994.

[20] F. Andrade, H. Sanca, F. Souza, P. Barra, "Comparative study of phasor estimation techniques applied on distance protection," IEEE Electrical Power and Energy Conference, 2023, doi: 10.1109/EPEC56903.2022.10000090.

[21] A. Zamora-Mendez, F. Zelaya, J. Serna, J. Chow, M. Paternina, "Model-based synchrophasor estimation by exploiting the eigensystem realization approach," *Electric Power Systems Research*, vol. 182, 2020, doi: 10.1016/j.epsr.2020.106249.

[22] S. Kang, D. Lee, S. Nam, P. Crossley, Y. Kang, "Fourier transform-based modified phasor estimation method immune to the effect of the DC offsets," *IEEE Transactions on Power Delivery*, vol. 24, no. 3, pp. 1104-1111, 2009, doi: 10.1109/TPWRD.2009.2014032.

[23] A. Yusuff, A. Jimoh, J. Munda, "Stationary wavelet transform and single differentiator based decaying DC-offset filtering in post fault measurements," *Measurment*, vol. 47, 2014, doi: 10.1016/j.measurement.2013.10.022.

[24] H. Hajizadeh, A. Ahmadi, M. Sanaye-Pasand, "An analytical fast decaying dc mitigation method for digital relaying applications," *IEEE Transactions on Power Delivery*, vol. 36, pp. 3529- 3537, 2021, doi: 10.1109/TPWRD.2020.3044376.

[25] A. Ghorbani, H. Mehrjerdi, M. Sanaye-Pasand, " An accurate non-pilot scheme for accelerated trip of distance relay zone-2 faults," *IEEE Transactions on Power Delivery*, vol. 36, n. 3, pp. 1370- 1379, 2020, doi: 10.1109/TPWRD.2020.3007559.

[26] M. Kalam, M. Jamil, "Wavelet-fuzzy based protection scheme of EHV-AC transmission system and efficacy of discrete Fourier transform," *Journal of Electrical Systems and Information Technology*, vol. 5, n. 3, pp. 371- 387, 2018, doi: 10.1016/j.jesit.2018.02.006.

[27] J. Lamber, A. Phadke, D. McNabb, "Accurate voltage phasor measurement in a series-compensated network," *IEEE Transactions on Power Delivery*, vol. 9, pp. 501-509, 1994, soi: 10.1109/61.277722.

[28] A. Phadke, *J. Thorp, Computer Relaying for Power Systems*, John Wiely & Sons, 2009.

[29] E. Vázquez, A. Zamora-Mendez, M. Paternina, L. Trujillo-Guajardo, J. Serna, "Dynamic phasor-driven digital distance relays protection," *Electric Power Systems Research*, vol. 184, 2020, doi: 10.1016/j.epsr.2020.106316.

[30] A. Rahmati, *R.* Adhami, "An accurate filtering technique to mitigate transient decaying dc offset, " *IEEE Transactions on Power Delivery*, vol. 29, pp. 966- 968, 2014, doi: 10.1109/TPWRD.2013.2288011.

[31] E. Rosolowski, J. Iżykowski, B. Kasztenny "Adaptive measuring algorithm suppressing a decaying DC component for digital protective relays," *Electric Power Systems Research*, vol. 60, 2001, doi: 10.1016/S0378-7796(01)00171-7.

[32] G. Jyh-Cherng, S. Yu, "Removal of dc offset in current and voltage signals using a novel fourier filter algorithm," *IEEE Transactions on Power Delivery*, vol. 15, pp. 73-79, 2000, doi: 10.1109/61.847231.

[33] M. Pazoki, "A new dc-offset removal method for distance-relaying application using intrinsic time-scale decomposition," *IEEE Transactions on Power Delivery*, vol. 33, pp. 971- 980, 2018, doi: 10.1109/TPWRD.2017.2728188.

[34] K. Min, S. Santoso, "DC offset removal algorithm for improving location estimates of momentary faults," *IEEE Transactions on Smart Grid*, vol. 9, pp. 5503-5511, 2018, doi: 10.1109/TSG.2017.2688981.

[35] H. Jalili, D. Yuqian, L. Yongli, W. Gang, L. Shanshan, "Distance relay protection based on artificial neural network," Fourth International Conference on Advances in Power System Control, Operation and Management, 1997, doi: 10.1049/cp:19971887.

[36] Y. Li, B. China, X. Zhang, J. He, "An ann-based distance protective relays of transmission lines," Seventh International Conference on Developments in Power System Protection, 2001, doi: 10.1049/cp:20010162.

[37] M. Tawfik, M. Morcos, "Ann based techniques for estimating fault location on transmission lines using prony method," *IEEE Transactions on Power Delivery,* vol. 16, pp. 219- 224, 2001, doi: 10.1109/61.915486.

[38] A. Abu-Elanien, M. Salama, "An ANN-based protection technique for MTDC systems with multiple configurations," *Alexandria Engineering Journal*, vol. 63, pp. 549-561, 2023, doi: 10.1016/j.aej.2022.08.018.

[39] Z. Wong, I. Chew, W. Wong, S. Sivakumar, F. Juwono, "Hybrid HVAC-HVDC grid fault detection & classification using ANN," 10th International Conference on Smart Computing and Communication, 2024, doi: 10.1109/ICSCC62041.2024.10690637.

[40] C. Silva, G. Junior, A. Morais, G. Marchesan, F. Guarda, "A continually online trained impedance estimation algorithm for transmission line distance protection tolerant to system frequency deviation," *Electric Power Systems Research*, vol. 147, 2017, doi: 10.1016/j.epsr.2017.02.023.

[41] R. Santos, E. Senger "Transmission lines distance protection using artificial neural networks," *International Journal of Electrical Power & Energy Systems*, vol. 33, 2011, doi: 10.1016/j.ijepes.2010.12.029.

[42] A. Ghorbani, H. Mehrjerdi, H. Heydari, S. Ghanimati, "A pilot protection algorithm for TCSC compensated transmission line with accurate fault location capability," *International Journal of Electrical Power & Energy Systems*, vol. 122, 2020, doi: 10.1016/j.ijepes.2020.106191.

[43] F. Rafique, L. Fu, R. Mai, "LSTM autoencoders based unsupervised machine learning for transmission line protection," *Electric Power Systems Research*, vol. 221, 2023, doi: 10.1016/j.epsr.2023.109432.

[44] G. Benmouyal, "Removal of dc-offset in current waveforms using digital mimic filtering," *IEEE Transactions on Power Delivery*, vol. 10, pp. 621-630, 1995, doi: 10.1109/61.400869.

[45] S. Ebrahimi, A. Ghorbani, "Performance comparison of LOE protection of synchronous generator in the presence of UPFC," *Engineering Science and Technology, an International Journal*, vol. 19, pp. 71-78, 2016, doi: 10.1016/j.jestch.2015.07.003.

[46] A. Ghorbani, S. Soleymani, B. Mozafari, "A PMU-based LOE protection of synchronous generator in the presence of GIPFC," *IEEE Transactions on Power Delivery*, vol. 31, pp. 551-558, 2015, doi: 10.1109/TPWRD.2015.2440314.

[47] A. Ghorbani, B. Mozafari, S. Soleymani, A. Ranjbar "Impact of STATCOM and SSSC on synchronous generator LOE protection," *Turkish Journal of Electrical Engineering and Computer Sciences*, vol. 24, pp. 2575-2588, 2016, doi: 10.3906/elk-1403-13.

[48] S. Nakamori, "Centralized Robust Multi-Sensor Chandrasekhar-Type Recursive Least-Squares Wiener Filter in Linear Discrete-Time Stochastic Systems with Uncertain Parameters," *Jordan Journal of Electrical Engineering*, vol. 7, n. 3, pp. 289-303, 2021, doi: 10.5455/jjee.204-1615182000.